

Transition rate for impact ionization in the approximation of a parabolic band structure

Jon Geist and Warren K. Gladden

Radiometric Physics Division, National Bureau of Standards, Washington, D.C. 20234

(Received 22 November 1982)

Recently, Alig, Bloom, and Struck have reported a simple model of ionization scattering in semiconductors and insulators. Their model is based upon the random- k approximation to the transition rate for impact ionization, and upon a generic band structure with only two free parameters to describe all materials. The present paper describes the first step in an attempt to understand in detail why such a simple model works so well. The random- k approximation to the transition rate for impact ionization is tested on a highly symmetric band-structure model for which most of the dimensions of the twelve-dimensional transition-rate integral can be treated analytically. The difference near threshold between the random- k approximation and the rigorous result can be much larger than indicated by Kane's Monte Carlo integration for the silicon band structure, but this difference seems to be unimportant in practical problems where impact ionization competes with phonon emission.

I. INTRODUCTION

Recently Alig, Bloom, and Struck¹ (ABS) were able to describe a large body of impact-ionization phenomena at high primary-particle energy on the basis of three simple assumptions. These are as follows: (1) The band structure of a semiconductor or insulator is approximated by two parabolas whose vertices are separated by the band-gap energy E_G , and whose effective masses are equal to the free-electron mass; (2) the transition rate for impact ionization is approximated by the random- k approximation; and (3) there is a threshold energy E_{th} below which impact ionization does not occur. Particles with energies above the plasmon energy E_p were assumed to deposit all of their energy in plasmons without loss, and E_{th} served as a cutoff energy to reflect the effect of the real band structure near threshold.

Within this framework, ABS could describe a variety of experimental results in terms of the parameters E_G , E_{th} , and a third parameter A which is proportional to the ratio of the average matrix element for impact ionization to that for phonon emission. Moreover, they found that a single value of A could be applied to both electrons and holes in a variety of materials over a wide range of particle energy E_i . ABS pointed out that this result is rather surprising. There is no obvious reason why the ratio of the matrix elements for electron-electron scattering should be proportional to those for electron-phonon scattering as a function of E_i . Nor is it obvious why this ratio should be independent of ma-

terial type. Clearly, it would be interesting to understand in detail why the very simple model of ABS works so well. This paper reports a first step in this direction: a reexamination of the random- k approximation.

The random- k approximation for $r(E_i)$, the transition rate for impact ionization by a particle of energy E_i , is itself rather puzzling. It effectively ignores momentum conservation, yet according to Kane,² it gives excellent agreement with a rigorous, momentum-conserving calculation of $r(E_i)$ based on the silicon band structure. The rigorous calculation is much more complicated than the random- k approximation. The latter involves a three-dimensional integral in energy space; the former involves a twelve-dimensional integral in k space, which Kane evaluated using a Monte Carlo procedure. As shown in Fig. 1, the only discernable difference between the results of the random- k approximation and the rigorous calculation is the statistical scatter inherent in the Monte Carlo procedure. The agreement spans almost 5 orders of magnitude, and is so excellent as to suggest that no approximation is involved.

In this paper we adopt the parabolic band structure of ABS and derive the rigorous expression for $r(E_i)$ consistent with this band structure. We then compare the low-energy behavior of this expression with that of the random- k approximation for the same band structure, and find large discrepancies very near threshold. While this contrasts strongly with the conclusion that Kane drew from his results on silicon, we find that it makes no difference when used in the model of ABS.

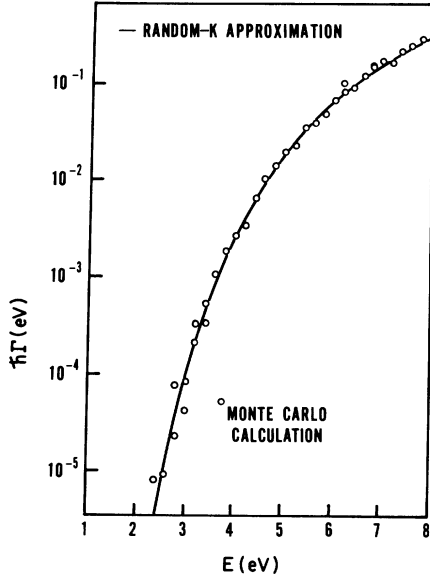


FIG. 1. Comparison of the random- k approximation to the transition rate for impact ionization in silicon with a Monte Carlo evaluation of the rigorous expression for the transition rate (after Kane). Γ is the transition rate when the primary electron has energy E with respect to the valence-band edge.

II. TRANSITION RATE FOR IMPACT IONIZATION

In Ref. 2 Kane considered the transition rate for an electron in the Bloch state $|E_c(\vec{k}_1)\rangle$ to scatter inelastically to the state $|E_c(\vec{k}_2)\rangle$ by creating an electron and hole in the states $|E_c(\vec{k}_3)\rangle$ and $|E_v(\vec{k}_4)\rangle$, respectively. Here the subscript c indi-

cates a conduction band, and the subscript v , a valence band. Kane averaged this transition rate over all \vec{k}_1 for which $E_c(\vec{k}_1) = E_1$. We write this average rate as

$$r = C \sum_{\vec{K}} \int \prod_{m=1}^4 d^3k_m \delta \left[\sum_{n=1}^4 a_n \vec{k}_n - \vec{K} \right] \delta(E_c(\vec{k}_1) - E_1) \times \delta \left[\sum_{n=1}^4 a_n E_x(\vec{k}_n) \right] |M|^2, \quad (1)$$

where $x = x(n)$ is c or v as appropriate, the sum over \vec{K} spans the space of reciprocal-lattice vectors, and M is the matrix element for the transition (including exchange). With $a_1 = a_4 = -a_2 = -a_3 = 1$, and

$$C = \frac{(2\pi/\hbar)[V/(2\pi)^3]^2}{\int d^3k_1 \delta(E_c(\vec{k}_1) - E_1)}, \quad (2)$$

Eq. (1) is the same equation studied by Kane, with minor differences in notation and form. For instance, we have adopted the extended-zone scheme, and have summed over all reciprocal-lattice vectors \vec{K} , whereas Kane used the reduced zone and summed over various band indexes.³ Also, we have multiplied the transition rate by $d^3k_4 \times \delta(\vec{k}_1 + \vec{k}_4 - \vec{k}_3 - \vec{k}_2 - \vec{K})$, and integrated over d^3k_4 to include momentum conservation within Eq. (1), rather than to carry it along as a subsidiary constraint as Kane did.⁴

In the Appendix to this paper, we show that most of the integrations indicated in Eqs. (1) and (2) can be carried out analytically for the parabolic band structure of ABS. After this is done and dimensionless variables are introduced, the transition rate can be written as

$$r(E_i) = M(E_i) \sum_{n=0}^{\infty} F_n(E_i), \quad (3)$$

$$M(E_i) = \left[\frac{2\pi |M|^2 V^2}{\hbar} \right] \frac{(2m/\hbar^2)^3 (E_i - E_G)^{5/2}}{16(2\pi)^4 E_i^{1/2}}, \quad (4)$$

$$F_0(E_i) = 2 \int_0^1 dx \int_0^{1-x} dy R\{\omega(\varepsilon, x, y)\}, \quad (5)$$

$$F_n(E_i) = \frac{N_n}{w_n} \int_0^1 dx \int_0^{1-x} dy \int_{|x^{1/2} - (1-x-y)^{1/2}|}^{x^{1/2} + (1-x-y)^{1/2}} du R\{\Omega(\varepsilon, u, w_n, y)\}, \quad (6)$$

$$\omega(\varepsilon, x, y) = \min\{\varepsilon^{1/2} + y^{1/2}, x^{1/2} + (1-x-y)^{1/2}\} - \max\{\varepsilon^{1/2} + y^{1/2}, |x^{1/2} - (1-x-y)^{1/2}|\}, \quad (7)$$

$$\Omega(\varepsilon, u, w, y) = [u^2 + w^2 + 2uw \min\{1, \alpha(\varepsilon, w)\}]^{1/2} - [u^2 + w^2 + 2uw \max\{-1, \beta(\varepsilon, w)\}]^{1/2}, \quad (8)$$

$$\alpha(\varepsilon, w) = [\varepsilon + y - u^2 - w^2 + 2(\varepsilon y)^{1/2}] / 2uw, \quad (9)$$

$$\beta(\varepsilon, w) = [\varepsilon + y - u^2 - w^2 - 2(\varepsilon y)^{1/2}] / 2uw, \quad (10)$$

$$w = (\hbar^2/2m)^{1/2} |\vec{K}| / (E_i - E_G)^{1/2}, \quad (11)$$

with $E_i = E_1 - E_G$, $\varepsilon = E_i / (E_i - E_G)$, and $R\{S\} = S$ for real $S > 0$, but is zero otherwise.

It is possible to replace the sum over the reciprocal-lattice vectors by a sum over the integers n because the \vec{K} vectors contribute to the sum in Eq. (1) only through their length. Thus they can be ordered according to their length. The quantities w_n and N_n are the values of w and the number of \vec{K} vectors associated with a given value of the ordering index n .

III. HYPOTHETICAL DIRECT-GAP BAND STRUCTURE

To make this concrete, consider the case where the primitive reciprocal-lattice vectors are given by $\vec{h} = (2\pi/a)(1, 1, -1)$ and its permutations, with $a = 0.543$ nm (the length of the cubic unit cell for silicon). Thus

$$\vec{K} = (2\pi/a)(n_2 + n_3 - n_1, n_3 + n_1 - n_2, n_1 + n_2 - n_3), \quad (12)$$

$$|\vec{K}| = (2\pi/a)\xi(n_1, n_2, n_3) = (2\pi/a)[n_1^2 + n_2^2 + n_3^2 + (n_1 - n_2)^2 + (n_2 - n_3)^2 + (n_3 - n_1)^2]^{1/2}, \quad (13)$$

and according to the definition of w in Eq. (11)

$$w_n = (\hbar^2/2m)^{1/2}(2\pi/a) \times \xi(n_1, n_2, n_3)(E_i - E_G)^{-1/2}, \quad (14)$$

where $n_1, n_2,$ and n_3 are integers, and where $n = n(n_1, n_2, n_3)$, $\xi(n_1, n_2, n_3)$, and N_n are tabulated in Table I for $n \leq 7$.

Notice that there is no contribution to the sum over n for a given value of n until $E_i > \hat{E}_i(n)$, the root of $\alpha(\epsilon, w(E_i(n))) = -1$. Otherwise, $\alpha(\epsilon, w) < -1$, and the $R\{S\}$ function is zero, because

$$\min[1, \alpha(\epsilon, w)] < \max[-1, \beta(\epsilon, w)]$$

in Eq. (8). To find $\hat{E}_i(n)$, set $\alpha(\epsilon, w) = -1$ in Eq. (9) and solve for the greater root \hat{w} . The result is

$$w = u + [\epsilon + y + 2(\epsilon y)^{1/2}]^{1/2}. \quad (15)$$

It is clear that for any given value of y , \hat{w} has its maximum value when u has its maximum value, namely $\hat{u} = x^{1/2} + (1-x-y)^{1/2}$. Set $\partial\hat{u}/\partial x = 0$ to see that \hat{u} has its maximum value as a function of y when $x = (1-y)/2$, that is, $\hat{u} = 2(1-y)^{1/2}$. Substitute this result into Eq. (15), let $y = \alpha^2\epsilon$, and set

TABLE I. Values of ξ_n , N_n , and $\hat{E}_i(n)$, the latter in eV, corresponding to the index n which orders the reciprocal-lattice vectors according to increasing length for a parabolic band, direct-gap semiconductor with the same lattice structure as silicon.

n	ξ_n	N_n	$\hat{E}_i(n)$
1	$3^{1/2}$	8	3.91
2	$4^{1/2}$	6	4.59
3	$8^{1/2}$	12	7.31
4	$11^{1/2}$	24	9.36
5	$12^{1/2}$	8	10.04
6	$16^{1/2}$	6	12.77
7	$19^{1/2}$	24	14.82

$\partial\hat{w}/\partial\alpha = 0$ to see that \hat{w} has its maximum value for $y = \frac{1}{3}$. $\hat{E}_i(n)$ is also listed in Table I.

We have used Eqs. (3)–(15) to evaluate $r(E_i)$ over the range between the thresholds for impact ionization and plasmon excitation in silicon. The numerical integrations were performed by dividing each integration interval into 25 subintervals, and approximating the average value of the integrand over each subinterval by its midinterval value. The results are shown in Fig. 2 for a primary electron with energy E measured from the top of the valence band. This choice was made in order to facilitate comparison with Kane's results shown in Fig. 1. The contribution from $\vec{K} = 0$, and from the other values of \vec{K} ,

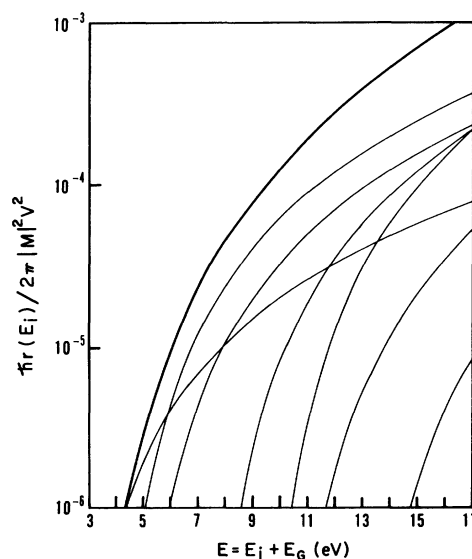


FIG. 2. Transition rate for impact ionization for a direct-gap, parabolic band structure in a hypothetical crystal structure with the same crystal structure and lattice constant as silicon. The contribution from the various reciprocal-lattice vectors grouped and indexed according to their lengths is also shown.

grouped and indexed according to their length, are also shown.

IV. INDIRECT GAP

The rigorous curve for $r(E_i)$ in Fig. 2 applies to a direct-gap, parabolic band structure in a hypothetical material with the same crystal structure and lattice constant as silicon. It is also interesting to consider an indirect-gap, parabolic band structure with all parameters identical to the direct-gap case except for the location of the conduction-band minimum. This change in band structure will change the requirements of momentum conservation, and so $r(E_i)$ will also change. On the other hand, this change in band structure leaves the density of states unchanged, so that the random- k approximation to $r(E_i)$ remains unchanged.

It is shown in the Appendix that the form of all of the Eqs. (3)–(11) can be retained under the transformation to an indirect gap. All that changes is the grouping, ordering, and indexing of the \vec{K} vectors according to their lengths. For instance, there is no reciprocal-lattice vector such that $\vec{K}=0$. Table II lists the values of ξ_n and N_n that apply to the indirect-gap structure with conduction-band minimum at $\vec{k}_0=(1,0,0)\pi/a$.

In reporting his momentum-conserving, Monte Carlo calculation of $r(E_i)$ for the silicon band structure, Kane² stated, "The delta functions are represented by rectangles of unit area and width 0.1 eV for the primary energy and 0.4 eV for energy conservation, so that energy conservation is satisfied to within ± 0.2 eV." To simulate the effect of not conserving energy in this way, let $\gamma = (0.2 \text{ eV})/(E_i - E_G)$, and replace $(1-x-y)^{1/2}$ by $(1-x-y)^{1/2} \pm \gamma$ in Eqs. (6) and (7), where the sign is chosen to maximize the values of the integrals in Eqs. (5) and (6). Specifically, replace $x^{1/2} + (1-x-y)^{1/2}$ by $x^{1/2} + (1-x-y)^{1/2} + \gamma$ and $|x^{1/2} - (1-x-y)^{1/2}|$ by the minimum of $|x^{1/2} - (1-x-y)^{1/2} - \gamma|$ and $|x^{1/2} - (1-x-y)^{1/2} + \gamma|$.

Figure 3 compares the ratios of $r(E_i)$ to the

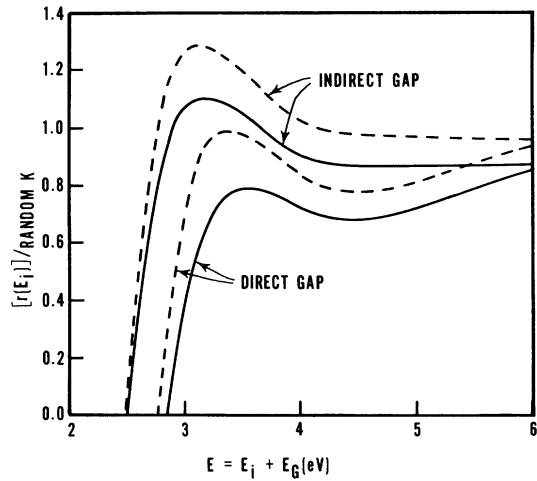


FIG. 3. Ratios of the rigorous transition rate to the random- k approximation for the hypothetical direct-gap and indirect-gap semiconductors considered in the text are shown with solid lines. The random- k approximation is identical for both cases because the density of states is the same for the direct- and indirect-gap band structures that were considered. The effect of relaxing energy conservation by ± 0.2 eV in the rigorous calculation is shown with dashed lines.

random- k approximation to $r(E_i)$ for the direct-gap and indirect-gap band structures described above, both with energy conservation ± 0.2 eV and with true energy conservation. Recall that the random- k approximation is the same for direct- and indirect-gap band structures having identical densities of states.

A number of interesting ideas are illustrated in Fig. 3. First, changing the band structure subject to the constraint that the density of states remains fixed can change the transition rate for impact ionization. Second, while Kane's Monte Carlo calculation for silicon suggests that the random- k approximation is about as accurate near threshold as at high energy, our results show that this is not necessarily the case. In this connection, our simulation of the way Kane violated conservation of energy by ± 0.2 eV in his Monte Carlo integration suggests that this is not the cause of the good agreement that he obtained down to below 2.5 eV, and that some other explanation is necessary. Perhaps it is a special property of the silicon band structure, or an artifact of some other approximations that Kane adopted in order to carry out what is an extremely difficult integration in a real band structure.

The possibility that the good agreement that Kane observed even below 2.5 eV is a special property of the silicon band structure should not be dismissed lightly. Figure 3 shows how much the agreement

TABLE II. Values of ξ_n and N_n as in Table I, except that the model semiconductor has an indirect gap as discussed in the text.

n	ξ_n	N_n
1	$3^{1/2}/2$	2
2	$11^{1/2}/2$	6
3	$19^{1/2}/2$	6
4	$27^{1/2}/2$	8
5	$35^{1/2}/2$	12

between the random- k approximation and the rigorous result improves in going from the case of a direct-gap to a particular indirect-gap band structure. Since this particular indirect-gap structure was chosen from all possible indirect structures merely for convenience, it is probable that indirect-gap structures exist for which the agreement is even better. Perhaps silicon is one of these. If Kane had tested the random- k approximation on the direct-gap semiconductors GaAs, rather than silicon, he probably would have found considerably worse agreement near threshold.

V. EFFECT ON MEASURABLE PROPERTIES

The preceding section emphasized the differences between the random- k approximation and a rigorous (momentum-conserving) calculation of the transition rate for impact ionization. This section will show that these differences, while real, are rather insignificant in their effect on observable impact-ionization phenomena.

First notice that $E_i + E_G = 2.24$ eV is the threshold for impact ionization in silicon that is determined by conservation of energy. The thresholds determined by momentum conservation occur at 2.5 and 2.8 eV, respectively, for the indirect- and direct-gap band structures that we considered. ABS used both the random- k approximation and an approximation that was equal to zero for $E_i + E_G < 2.8$ eV, but equal to the random- k approximation for $E_i + E_G > 2.8$ eV. These two approximations produced different results when phonon emission was ignored, but produced identical results when the ratio of the average matrix element for phonon emission to that for impact ionization was chosen to give the experimentally determined average pair creation energy in silicon.

In other words, impact ionization is completely negligible compared to phonon emission below 2.8 eV, so it does not make any difference what the transition rate for impact ionization is in this region as long as it does not increase with decreasing particle energy. Thus pair production by energetic particles is not even affected by the transition rate near threshold where the differences between the random- k approximation and the rigorous results are the greatest. Furthermore, as shown in Fig. 3, the differences among the random- k approximation and the various rigorous results are rather insignificant above 6 eV.

Now consider the changes if ABS had used the rigorous, direct-gap transition rate rather than the random- k approximation in their calculations. They used both $r(E_i)$ and the transition rate for phonon emission $r'(E_i)$ in a recursion relation to calculate

$p_0(E_i)$, the probability that a particle with kinetic energy E_i loses its energy to phonons without causing an impact ionization. Then $p_0(E_i)$, $r(E_i)$, and $r'(E_i)$ were used in another recursion relation to calculate $p_n(E_i)$, the probability of creating exactly n electron-hole pairs. All of the experimentally accessible parameters were then calculated from the $p_n(E_i)$.

Figure 4 shows the $p_0(E_i)$ curve that ABS obtained using the random- k approximation to $r(E_i)$. The important point is that below 3 eV and above 6 eV, $p_0(E_i)$ is given by the asymptotic values 1 and 0, respectively. Thus $p_0(E_i)$ is unaffected by changes in $r(E_i)$ that occur outside the (3–6)-eV region. This point was already made with respect to the near threshold values of $r(E_i)$.

If ABS had used the rigorous curve, they would have chosen the value of the A parameter so that their calculation gave the correct average pair production energy ϵ for silicon. This is equivalent to holding A fixed but translating the rigorous result for $r(E_i)$ vertically until it gives the correct value of ϵ . To produce a new $p_0(E_i)$ curve that oscillates about the one shown in Fig. 4, a translation of about 25% would be needed. However, this would systematically increase all of the $p_n(E_i)$, for $n=1,2,3,\dots$, relative to their values as determined by the random- k approximation, thereby increasing ϵ too much. This analysis indicates that A need be increased no more than $10\% \pm 10\%$ in order to produce the correct value of ϵ . The changes that this change in A would produce in $p_0(E)$ can now be considered.

Figure 5 compares the actual values of the rigorous, direct-gap transition rate with the random- k approximation in the (3–6)-eV region. Notice that a shift of the random- k curve to higher energy by about 1.5 eV will cause the two curves to

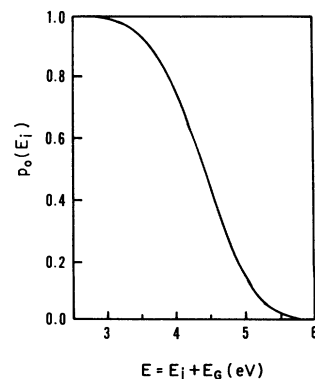


FIG. 4. Probability that a carrier with kinetic energy E_i will cause no impact ionizations before relaxing to the band edge.

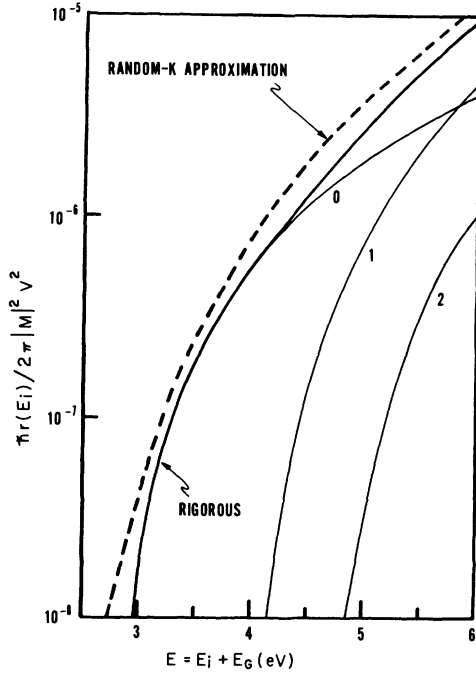


FIG. 5. Comparison of the random- k approximation and the rigorous transition rate near threshold for the direct-gap band structure considered in the text.

oscillate around each other. The steeper slope near threshold more than compensates for the better agreement at higher energy, and so the fit resulting from translation along the energy axis is better than might be expected from Fig. 3. Thus we can expect the rigorous transition rate to produce a new $p_0(E_i)$ whose shape has minor oscillations about that shown in Fig. 5, and whose position is displaced by about 0.7 ± 0.7 eV toward higher energy. The changes in $p_n(E_i)$ for $n > 0$ are not so easily analyzed. However, they can be expected to be of comparable or smaller magnitude. It depends upon the relative importance of the various $p_n(E_i)$ determining ϵ .

Changes in $p_n(E_i)$ of the nature just described cannot have large effects on measurable quantities such as $\langle n(E_i) \rangle$, the average number of electron-hole pairs created by an energetic primary particle with kinetic energy E_i . From Eq. (1) of ABS and the requirement that

$$\sum_{n=0}^{\infty} p_n(E_i) = 1, \quad (16)$$

it is easy to show that

$$\langle n(E_i) \rangle = 1 - p_0(E_i) + \sum_{n=2}^{\infty} (n-1)p_n(E_i) \quad (17)$$

for E_i less than the plasmon excitation threshold

16.6 eV. Thus the changes in $p_0(E_i)$ caused by different transition rates are directly reflected in $\langle n(E_i) \rangle$ in the (3–6)-eV region.

ABS have shown that the pair creation energy $E_i/\langle n(E_i) \rangle$ is very close to $\epsilon_k(E_p)$, the pair creation energy with plasmon intervention when $E_i = E_p$, even when E_i is as small as 10 eV. This imposes the constraint concerning the correct value of ϵ directly on the $p_n(E_i)$ that contributes to $\langle n(E_i) \rangle$ for E_i less than the plasmon threshold. As a result, there is very little freedom for variations in $\langle n(E_i) \rangle$. The threshold can be shifted to higher energy by no more than about 0.5 eV, and little more than oscillations about the random- k approximation to $\langle n(E_i) \rangle$ can be tolerated at higher energies. In summary, while our results indicate small modifications to the detailed conclusions reported by Kane concerning the random- k approximation, Kane's major conclusion that it is an extremely powerful and accurate technique for studying impact-ionization phenomena is fully supported.

APPENDIX

In this appendix we show that many of the integrations indicated in Eq. (1) can be carried out analytically for the parabolic band structure of ABS, and we transform the partially integrated expression for the transition rate into a form that is convenient for numerical integration of the remaining integrals. Motivated by the random- k approximation, we rewrite Eq. (1) in terms of an integral over particle energies by multiplying Eq. (1) by

$$dE_2 \delta(E_c(\vec{k}_2) - E_2) dE_3 \delta(E_c(\vec{k}_3) - E_3) \\ \times dE_4 \delta(E_v(\vec{k}_4) - E_4)$$

and integrating over $dE_2 dE_3 dE_4$. Next, we assume that $|M|^2$ has no explicit dependence upon the \vec{k}_n , but only implicit dependence through the $E_x(\vec{k}_n)$, and repeatedly apply the δ -function theorem.

$$\int \delta(f(x) - u) g(f(x)) dx = \int \delta(f(x) - u) g(u) dx \quad (A1)$$

to systematically replace $E_x(\vec{k}_n)$ by E_n in both $|M|^2$ and the δ function coupling the $E_x(\vec{k}_n)$. The result can be written as

$$r = C \int dE_2 dE_3 dE_4 \delta \left(\sum_{n=1}^4 a_n E_n \right) |M|^2 F, \quad (A2)$$

where

$$F = \sum_{\vec{K}} \int \prod_{m=1}^4 d^3k_m \delta(E_x(\vec{k}_m) - E_m) \times \delta \left[\sum_{n=1}^4 a_n \vec{k}_n - \vec{K} \right]. \quad (\text{A3})$$

In order to treat the parabolic bands that ABS considered, it will prove useful to integrate Eq. (A3) over d^3k_1 to remove the δ function in the particle quasimomenta, then to let $\vec{k} = \vec{k}_3 - \vec{k}_4$, and to rewrite the result in the form

$$F = \sum_{\vec{K}} \int d^3k L_{eh}(\vec{k}) L_{if}(\vec{k} + \vec{K}), \quad (\text{A4})$$

$$L_{eh}(\vec{k}) = \int d^3k_4 \delta(E_v(\vec{k}_4) + E_h) \times \delta(E_c(\vec{k}_4 + \vec{k}) - E_G - E_e), \quad (\text{A5})$$

$$L_{if}(\vec{k} + \vec{K}) = \int d^3k_2 \delta(E_c(\vec{k}_2) - E_G - E_f) \times \delta(E_c(\vec{k}_2 + \vec{k} + \vec{K}) - E_G - E_i). \quad (\text{A6})$$

$$L_{eh}(k) = \int_l dl \{ |\vec{\nabla}_4 E_v(\vec{k}_4)|^2 |\vec{\nabla}_4 E_c(\vec{k}_4 + \vec{k})|^2 - [\vec{\nabla}_4 E_v(\vec{k}_4) \cdot \vec{\nabla}_4 E_c(\vec{k}_4 + \vec{k})] \}^{1/2}, \quad (\text{A9})$$

where l is the circle of intersection of the surfaces $E_v(\vec{k}_4) + E_h = 0$ and $E_c(\vec{k}_4 + \vec{k}) - E_G - E_e = 0$.

Reference to Fig. 6 shows that the integrand is symmetric with respect to rotation about the \vec{k} axis. Thus all that is necessary to evaluate the integral is to multiply the circumference l of the circle of intersection by the integrand evaluated at some point on l . Evaluation of the integrand using Eqs. (A7) and (A8) is straightforward. The result can be put in the form

$$[4(\hbar^2/2m)^2 |\vec{k}_4| |\vec{k}| \sin\theta_4]^{-1}.$$

Figure 6 also shows that $l = 2\pi |\vec{k}_4| \sin\theta_4$. Thus

$$L_{eh}(\vec{k}) = (2\pi/4)(2m/\hbar^2)^2 |\vec{k}|^{-1} \quad (\text{A10})$$

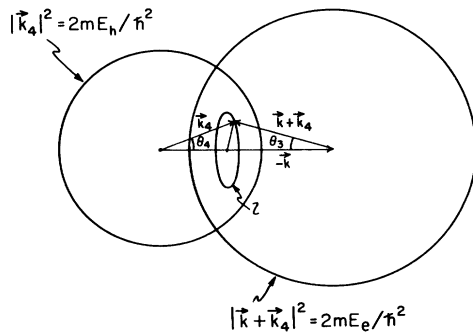


FIG. 6. Intersection of the spherical surfaces described by $|\vec{k}_4|^2 = 2mE_h/\hbar^2$ and $|\vec{k} + \vec{k}_4|^2 = 2mE_e/\hbar^2$.

In writing Eqs. (A4)–(A6) we have adopted the notation of ABS, wherein the particle energies are reported as kinetic energies. That is, $E_i = E_1 - E_G$, $E_f = E_2 - E_G$, $E_e = E_3 - E_G$, and $E_h = -E_4$. The subscripts i and f refer to the initial and final states of the primary scattering particle while e and h refer to the electron and hole created by the scattering event. This treats the particles more symmetrically in that all particle energies are positive, starting from zero at the band edge.

Next we will show that the integrations indicated in Eqs. (A5) and (A6) and some of those indicated in Eq. (A4) can be carried out analytically for the parabolic band structure of ABS. Specifically, let

$$E_c(\vec{k}) = (\hbar^2/2m) |\vec{k}|^2 + E_G, \quad (\text{A7})$$

$$E_v(k) = -(\hbar^2/2m) |\vec{k}|^2. \quad (\text{A8})$$

To integrate Eq. (A5) using Eqs. (A7) and (A8), convert the volume integral to the equivalent line integral

for

$$|E_e^{1/2} - E_h^{1/2}| \leq (\hbar^2/2m)^{1/2} |\vec{k}| \leq E_e^{1/2} + E_h^{1/2}. \quad (\text{A11})$$

When $|\vec{k}|$ is outside the bounds set by Eq. (A11), the two spherical surfaces shown in Fig. 6 do not intersect at all and $L_{eh}(\vec{k}) = 0$. Similarly,

$$L_{if}(\vec{k} + \vec{K}) = (2\pi/4)(2m/\hbar^2)^2 |\vec{k} + \vec{K}|^{-1} \quad (\text{A12})$$

for

$$E_i^{1/2} - E_f^{1/2} \leq (\hbar^2/2m)^{1/2} |\vec{k} + \vec{K}| \leq E_i^{1/2} + E_f^{1/2}, \quad (\text{A13})$$

and $L_{if}(\vec{k} + \vec{K}) = 0$ otherwise.

Now substitute Eqs. (A10) and (A12) into Eq. (A4) and convert the integral to spherical \vec{k} coordinates whose polar axis is parallel to \vec{K} , and let $k = |\vec{k}|$ and $K = |\vec{K}|$. Therefore,

$$F = \left[\frac{2\pi}{4} \right]^2 \left[\frac{2m}{\hbar^2} \right]^4 \times \sum_{\vec{K}} \int_0^{2\pi} d\phi \int \frac{dk k d\theta \sin\theta}{(k^2 + K^2 + 2kK \cos\theta)^{1/2}}, \quad (\text{A14})$$

where the limits of integration for k are determined by Eq. (A11), and the limits of integration for θ are determined by

$$E_i^{1/2} - E_f^{1/2} \leq (\hbar^2/2m)^{1/2} (k^2 + K^2 + 2kK \cos\theta)^{1/2} \leq E_i^{1/2} + E_f^{1/2} \quad (\text{A15})$$

and the requirement that $\cos\theta$ lie between -1 and 1 .

The term with $\vec{K}=0$ must be integrated separately from the other terms because Eq. (A15) does not limit θ in this particular case. Instead, the limits of integration for k are the minimum of the upper limits and the maximum of the lower limits in Eqs. (A11) and (A15). For $\vec{K}=0$, the integrations over θ , ϕ , and k can all be carried out analytically. However, for $\vec{K} \neq 0$, one of the integrations, over either θ or k , must be carried out numerically; let it be k . When these results are substituted into Eq. (A2), one of the indicated integrations, let it be that with respect to E_h , can be carried out analytically, but the remaining two must be treated numerically. At this point the formulas become considerably more compact in terms of the dimensionless notation where $\varepsilon = E_i/(E_i - E_G)$, $x = E_e/(E_i - E_G)$, $y = E_f/$

$(E_i - E_G)$, $u = (\hbar^2/2m)^{1/2} k/(E_i - E_G)^{1/2}$, and $w = (\hbar^2/2m)^{1/2} K/(E_i - E_G)^{1/2}$. The final result can then be put in the form indicated by Eqs. (3)–(11) of the main text.

Now consider the case of an indirect-gap material with parabolic bands. For convenience, assume that the band minimum occurs at $\vec{k}_0 = (100)\pi/a$, and replace Eq. (A7) by

$$E_c(\vec{k}) = (\hbar^2/2m) |\vec{k} - \vec{k}_0|^2 + E_G. \quad (\text{A16})$$

This replaces \vec{k} by $\vec{k}' = \vec{k} - \vec{k}_0$ in Eqs. (A10) and (A11), so the form of these equations remains unchanged under this change of variable. The form of Eqs. (A14) and (A15) can also be retained by transforming to the new variables $\vec{k}' = \vec{k} - \vec{k}_0$ and $\vec{K}' = \vec{K} + \vec{k}_0$ in Eqs. (A12) and (A13). Thus everything remains the same, except the grouping, ordering, and indexing of the K' vectors according to their lengths.

¹R. C. Alig, S. Bloom, and C. W. Struck, Phys. Rev. B **22**, 5565 (1980).

²E. O. Kane, Phys. Rev. **159**, 624 (1967).

³We do not explicitly indicate any remaining summation over v and c needed due to degeneracy.

⁴Of course, the matrix elements actually are responsible for conserving momentum, but since we will follow

Kane and introduce an average over the nonzero matrix elements, it is necessary to explicitly conserve momentum. It turns out to be more convenient to introduce the conservation of momentum constraints by integration over the δ function rather than by direct substitution (to which, of course, it is equivalent).